

Shape coexistence in neutron-deficient Pb nuclei probed by quadrupole moment measurements

M. Ionescu-Bujor^a, A. Iordachescu^a, N. Mărginean^{a,b}, C.A. Ur^{a,c},
D. Bucurescu^a, G. Suliman^a, D.L. Balabanski^{d,e}, F. Brandolini^c,
S. Chmel^f, P. Detistov^g, K.A. Gladnishki^{d,g}, H. Hübel^f,
S. Mallion^h, R. Mărginean^c, N.H. Medinaⁱ, G. Neyens^h, P. Pavan^c,
R.V. Ribasⁱ, C. Rusu^b, K. Turzó^h, N. Vermeulen^h

^aNational Institute for Physics and Nuclear Engineering, Bucharest, Romania

^bINFN, Laboratori Nazionali di Legnaro, Legnaro, Italy

^cDipartimento di Fisica dell' Università and INFN, Padova, Italy

^dUniversità di Camerino and INFN Perugia, Italy

^eINRNE, Bulgarian Academy of Sciences, Sofia, Bulgaria

^fHelmholtz-Institute für Strahlen- und Kernphysik, Universität Bonn, Germany

^gSt. Kliment's Ohridsky University of Sofia, Sofia, Bulgaria

^hKatholieke Universiteit Leuven, Leuven, Belgium

ⁱInstituto de Física, Universidade de São Paulo, São Paulo, Brazil

Abstract

The spectroscopic quadrupole moments of the 11^- and 12^+ isomers in $^{192,194}\text{Pb}$, described by the $3s_{1/2}^{-2}1h_{9/2}1i_{13/2}$ intruder two-proton and $1i_{13/2}^2$ two-quasineutron configurations, respectively, have been investigated by the method of time-differential observation of the γ -ray perturbed angular distribution. The derived values are $|Q_s|(12^+, ^{192}\text{Pb}) = 0.32(4)$ eb, $|Q_s|(11^-, ^{192}\text{Pb}) = 2.9(3)$ eb and $|Q_s|(11^-, ^{194}\text{Pb}) = 3.6(4)$ eb. The 8^+ 2304 keV and 9^- 2514 keV states in ^{192}Pb have been identified as isomers, with half-lives of 3.9(3) and 3.3(3) ns, respectively. The experimental spectroscopic quadrupole moments for the 11^- and 12^+ isomers in neutron deficient Pb nuclei have been described in the frame of the pairing plus quadrupole model. The intrinsic quadrupole moments and deformation of the 11^- isomers are compared with the predictions of mean-field and interacting boson models.

Key words: Spectroscopic quadrupole moment; Shape coexistence

PACS: : 21.10.Ky, 21.60.Cs, 21.60.Ev, 27.80.+w

Neutron-deficient Pb isotopes are important benchmarks for investigating the phenomenon of shape coexistence in nuclei and have recently been the subject of much

experimental and theoretical interest. As a result of the shell closure at $Z=82$, they are spherical in the ground state, but the interplay between single-particle motion, collectivity, and pairing leads to a rich variety of coexisting structures at relatively low energies [1, 2]. The observation of low-lying excited 0^+ states is one of the essential experimental fingerprints. Detailed α - and β^+ /electron capture-decay studies have evidenced the systematic presence of such states in all even-even Pb isotopes between $A=184$ and $A=200$ [3, 4]. On the other hand, information concerning low-lying rotational bands was provided by in-beam studies using fusion-evaporation reactions [5–8]. A spectacular situation is offered by the neutron midshell $N=104$ nucleus ^{186}Pb , with the spherical ground-state and two lowest excited 0^+ states of prolate and oblate deformation [4]. The triple-shape coexistence in this nucleus was confirmed in very recent in-beam spectroscopic and lifetime studies [7, 8].

The theoretical investigation of the shape coexistence in the Pb region makes use of two complementary approaches. In the shell-model approach, the deformed states in Pb nuclei are associated with multi-particle multi-hole ($mp - mh$) proton excitations across the $Z=82$ gap [1]. The excitation energies of the intruder states are lowered by the residual proton-neutron interaction. Deformed oblate and prolate shapes are associated in this description with proton $2p - 2h$ and $4p - 4h$ intruder configurations, respectively. The proton particle-hole excitations cannot be easily handled in full-scale shell model calculations, therefore they are treated in the framework of algebraic models, such as the interaction boson model (IBM) [9]. In a very different picture, calculations using a deformed mean-field approach show the coexistence of energy minima of different shapes [12]. Several variants of the self-consistent mean-field method have been developed using either a Skyrme [13] or a Gogny [14] interaction. Detailed treatments including configuration mixing have been recently performed within both mean-field [13] and IBM [10, 11] to calculate excitation energies as well as quadrupole moments of the coexisting states.

An interesting feature of the Pb nuclei is that the shape coexistence shows up also in the presence of isomeric states involving quasiparticle excitations. In the even-mass $^{188-196}\text{Pb}$ isotopes, spherical high-spin isomeric states described by two-quasineutron configurations are coexisting with 11^- isomers involving the $2p - 2h$ $\pi 3s_{1/2}^{-2} 1h_{9/2} 1i_{13/2}$ intruder configuration. Enhanced $E3$ transitions from the 11^- isomers, with strengths in the range 20-30 W.u., were recently reported in $^{190-196}\text{Pb}$ by Dracoulis et al. [15, 16] and interpreted as an evidence that these states are oblate-deformed.

The coexisting isomeric states in Pb offer the opportunity to investigate their static quadrupole moments and therefore to provide direct fingerprints for nuclear shape coexistence. Such moments were reported in $^{194-200}\text{Pb}$ for the 12^+ isomeric states described by the $1i_{13/2}^2$ two-quasineutron configuration and rather small values, $Q_s \leq 0.8$ eb, were found, pointing to almost spherical shapes [17, 18]. As concerns the intruder 11^- isomers, spectroscopic quadrupole moments have been recently measured in $^{194,196}\text{Pb}$ by applying the level mixing spectroscopy (LEMS) tech-

nique [19, 20] and much higher values (*e. g.* $|Q_s|(11^-, ^{196}\text{Pb})=3.6(6) \text{ eb}$ [19, 21]) have been reported, indicating a larger deformation associated with the intruder excitation. The aim of the present work was to extend the experimental information about static moments of coexisting states in light Pb nuclei, for a detailed comparison with the theoretical predictions.

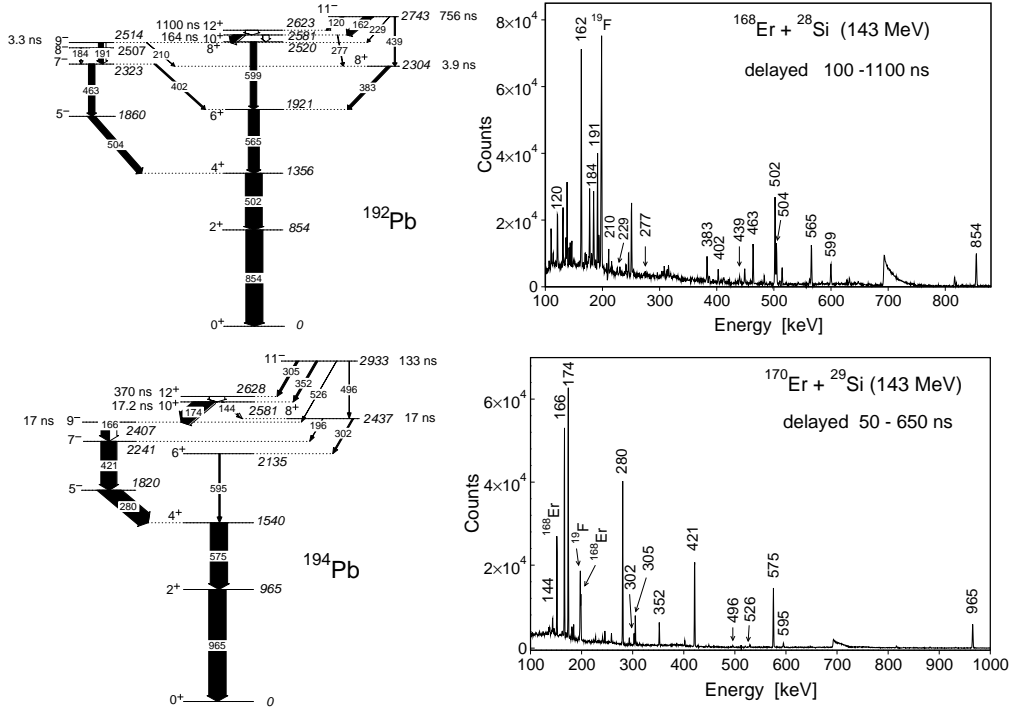


Fig. 1. Left: Partial level schemes showing the decay of isomeric states in ^{192}Pb [15, 22] and ^{194}Pb [16, 23]. The arrow widths are proportional with the population yields of the 11^- and 12^+ isomers determined in the present experiment. The isomer half-lives are from published data, excepting those of the 8^+ and 9^- states in ^{192}Pb which are from the present work. Right: Delayed spectra corrected for the background due to long-lived activities, registered with a HPGe detector. The delayed transitions belonging to ^{192}Pb (upper spectrum) and ^{194}Pb (lower spectrum) are labeled by energies.

The isomeric states were populated and aligned in the $^{168}\text{Er}(^{28}\text{Si},4n)^{192}\text{Pb}$ and $^{170}\text{Er}(^{29}\text{Si},5n)^{194}\text{Pb}$ reactions at the beam energy of 143 MeV. The beams, delivered by the Legnaro XTU-Tandem accelerator, were pulsed with 2 ns pulse width and a separation of $3.2 \mu\text{s}$ for ^{192}Pb and $1.6 \mu\text{s}$ for ^{194}Pb . The method of time-differential observation of the perturbed angular distribution (TDPAD) of deexciting γ -rays has been applied. The quadrupole interaction of the isomeric states has been investigated in the electric field gradient (EFG) of the polycrystalline lattice of metallic Bi in which they were in-beam implanted. For this purpose a layer of 5 mg/cm^2 metallic Bi has been evaporated on the rear side of the targets consisting of 0.5 mg/cm^2 metallic Er foils, enriched to 95.6% and 97.2% in ^{168}Er and ^{170}Er , respectively. A 50 mg/cm^2 foil of Pb was used as backing in order to stop the Si

projectiles and to prevent Bi oxidation. Planar HPGe detectors placed at the angles 0° and 90° with respect to the beam direction, and 20% efficiency HPGe detectors placed at the angles 27° and 90° with respect to the beam direction, were used to detect the γ rays. The time resolution for the planar detectors was about 10 ns and 7 ns at energies of 200 keV and 550 keV, respectively. For the detectors of 20% efficiency the time resolution at 550 keV was about 10 ns.

In the off-line analysis of list-mode data, two-dimensional matrices of energy versus time were formed for each detector. From these matrices time-gated energy spectra and energy-gated time spectra were constructed. The analysis of γ -ray intensities obtained from energy spectra coincident with the beam pulse (prompt spectra) and with various time intervals in-between the pulses (delayed spectra) provided information on the isomer population yields and on the branchings at different levels. The direct population of the 12^+ isomeric state in ^{194}Pb was found dominant, representing $\approx 60\%$ from the reaction channel, while that of the 11^- isomeric state was ≈ 3 times weaker. In ^{192}Pb the two isomeric states were populated almost equally, each with a cross section of about 30% from the reaction channel. Partial level schemes showing the isomeric decays and illustrative delayed γ spectra are shown in Fig. 1. The level scheme of ^{192}Pb includes a new weak decay, namely the 229 keV transition connecting the 11^- isomer at 2743 keV to the 2514 keV 9^- state. It is worthwhile to mention that very weak $11^- \rightarrow 9^-$ transitions were recently observed also in $^{194,196}\text{Pb}$ [16].

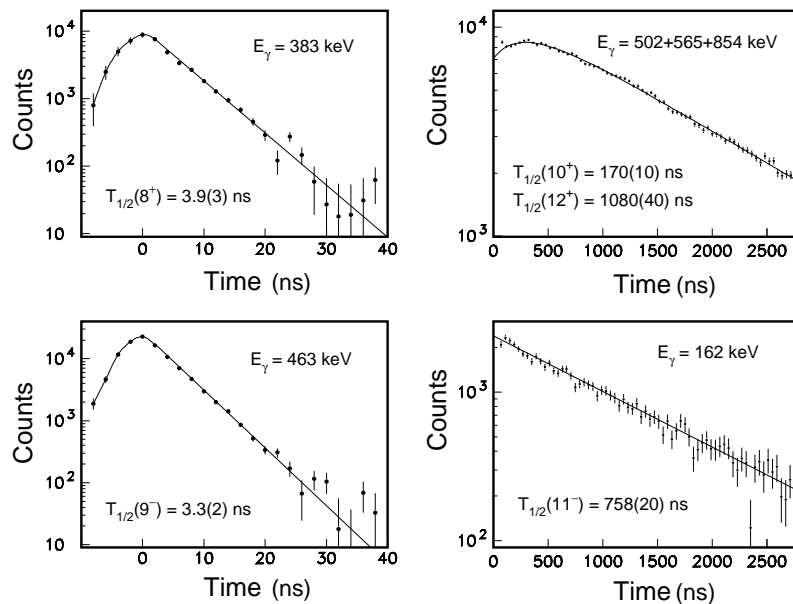


Fig. 2. Time spectra for selected delayed transitions in ^{192}Pb , registered with a HPGe detector. The prompt background and the contributions due to long-lived activities have been subtracted.

Lifetimes of the isomeric levels were determined from the analysis of time spectra for selected delayed γ rays. Illustrative time spectra obtained for ^{192}Pb are presented in Fig. 2. The half-lives of the known isomers were found in agreement with previ-

Table 1

$E2$ transition strengths determined in this work (^{192}Pb) and in Refs. [16, 23] (^{194}Pb), [16, 24] (^{196}Pb), [25] (^{198}Pb) and [26] (^{200}Pb).

$I_i^\pi \rightarrow I_f^\pi$	A	E_x^i (keV)	$T_{1/2}$ (ns)	E_γ (keV)	I_γ (%)	α_T	$B(E2)$ (W.u.)
$11^- \rightarrow 9^-$	192	2743	756(20)	229	1.2(3)	0.274	$1.7(5)\times 10^{-4}$
	194	2933	138(7)	526	1.1(3)	0.026	$1.6(4)\times 10^{-5}$
	196	3193	57(3)	884	2.1(3)	0.009	$5.5(8)\times 10^{-6}$
$8^+ \rightarrow 6^+$	192	2304	3.9(2)	383	100	0.058	0.25(3)
	194	2437	17(4)	302.5	0.81(3)	0.114	0.14(4)
$9^- \rightarrow 7^-$	192	2514	3.3(2)	191	88(2)	0.509	5.9(5)
	194	2407	17(3)	166	100	0.846	2.1(4)
	196	2308	52(5)	138.4	100	1.70	1.17(12)
	198	2231	137(10)	90	100	10.1	0.92(8)
	200	2183	424(10)	29.5	100	2100	0.43(1)

ously reported data for both ^{192}Pb [15, 22] and ^{194}Pb [16, 23]. In addition, short-lived components were found for the transitions depopulating the 8^+ 2304 keV and 9^- 2514 keV states in ^{192}Pb , and half-lives of 3.9(3) ns and 3.3(3) ns, respectively, have been determined. With the new isomeric decays identified in ^{192}Pb the systematics of $B(E2)$ values in light Pb nuclei has been extended, as seen in Table 1. The extremely low $B(E2)$ values for the transitions deexciting the 11^- states described by the two-proton intruder configuration are consistent with the large configuration change, the 9^- states involving predominantly the $2f_{5/2}^{-1}1i_{13/2}^{-1}$ two-neutron configuration [16]. On the other hand, the $E2$ transition from the 8^+ state described also as an intruder two-proton excitation [16] is not so hindered, indicating large admixtures of deformed proton intruder configurations in the structure of the 6^+ state. An increase of the mixing is expected when going toward lighter Pb isotopes, as discussed in [27]. This is supported by the experimental $B(E2)$ values which increase with the decrease of the neutron number. The same trend is observed also for the $9^- \rightarrow 7^-$ transition strength, pointing to an increased collectivity when approaching the neutron midshell.

The time spectra, background subtracted and normalized, were used to construct the experimental ratios $R_{exp}(t) = [I(t, \theta_1) - I(t, \theta_2)]/[I(t, \theta_1) - I(t, \theta_2)]$, where $\theta_1=0^\circ$ or 27° , and $\theta_2=90^\circ$. They were least-squares fitted to the expression:

$$R_{theo}(t) = \frac{3}{4}A_2 \sum s_{2n} \cos(n\omega_0 t) \quad (1)$$

with the angular distribution coefficient A_2 and the quadrupole interaction frequency $\omega_o = 2\pi/T_0$ as free parameters. The spin-dependent s_{2n} coefficients in the

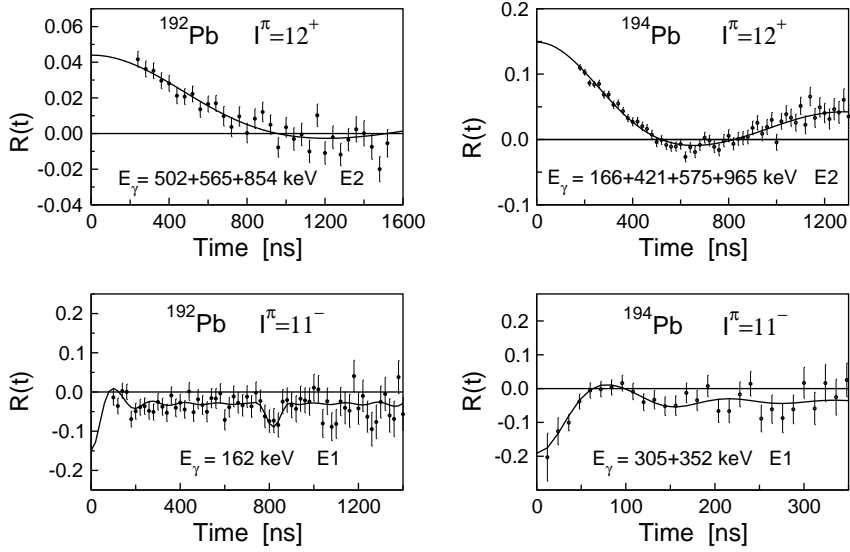


Fig. 3. TDPAD spectra showing the quadrupole interaction of the 11^- and 12^+ isomeric states in $^{192,194}\text{Pb}$ nuclei implanted in the polycrystalline lattice of metallic Bi.

theoretical expression (1) are tabulated in ref. [29] for an axially symmetric randomly oriented EFG. For an integer spin the modulation spectra are periodic with the basic repetition quadrupole period T_0 given by $T_0 = 4I(2I - 1)/3\nu_Q$, where $\nu_Q = Q_s V_{zz}/h$ is the quadrupole coupling constant depending on the spectroscopic quadrupole moment Q_s and the EFG strength V_{zz} . To determine the quadrupole interaction of the 11^- states the deexciting $E1$ transitions of 162 keV in ^{192}Pb and of 302+352 keV in ^{194}Pb , have been analysed. For the 12^+ states the dominant $E2$ transitions present in the decay have been considered. Illustrative experimental ratios are shown in Fig. 3 together with the appropriate least-squares fits. In the case of the 12^+ isomers, due to their weak quadrupole interaction strength, only the structure at the beginning of the modulation pattern could be observed in the TDPAD spectra. The 11^- isomers have been found to experience a much stronger interaction. The longer lifetime of this isomer in ^{192}Pb allowed to see the peak at $T_0/4$ in the modulation pattern. We note that while the 11^- isomers are subject to a single quadrupole interaction, the perturbation of the transitions used for the 12^+ states is more complex due to the presence of cascade isomers. The population component from the 11^- isomer is subject to a superposition of two interactions producing a smearing-out of the perturbation pattern. The isotropic behaviour of this component has as effect the reducing of the observed "effective" angular distribution coefficient, as observed experimentally in the TDPAD spectra of Fig. 3. The reduction is stronger in ^{192}Pb , where the component from the 11^- state is larger, as mentioned before. To analyse the perturbation of the side component of the 12^+ state one has to take into account also the other isomers present in the decay scheme (see Fig. 1). This was important in the case of ^{192}Pb , due to the longer lifetime of the 10^+ isomer (see Fig. 1). The theoretical curve was calculated by

applying a two-level formalism [30], with lifetimes and relative feeding of the 12^+ and 10^+ isomers taken from the analysis of the growth-decay curve (see Fig 2). The perturbation due to the shorter-lived states was found negligible.

The deduced ν_Q values were 96(6) and 10.6(11) MHz for the 11^- and 12^+ states in ^{192}Pb , respectively, and 120(8) and 16.2(6) MHz for the corresponding states in ^{194}Pb . Using the known quadrupole moment $|Q_s|(12^+, ^{194}\text{Pb}) = 0.48(3)$ eb [18], a reliable calibration of the electric field gradient for Pb in the Bi crystalline lattice, $V_{zz}(\text{PbBi}) = 1.39(10) \times 10^{21}$ V/m², has been derived in the present experiment. With this calibration, absolute values for spectroscopic quadrupole moments Q_s were obtained for the isomers in ^{192}Pb as $|Q_s|(12^+, ^{192}\text{Pb}) = 0.32(4)$ eb and $|Q_s|(11^-, ^{192}\text{Pb}) = 2.9(3)$ eb. For the 11^- isomer in ^{194}Pb a value of $|Q_s|(11^-, ^{194}\text{Pb}) = 3.6(4)$ eb has been deduced, in fair accordance with the previously reported value of 4.8(7) eb, derived with the LEMS method by applying a double perturbation analysis [20,21].

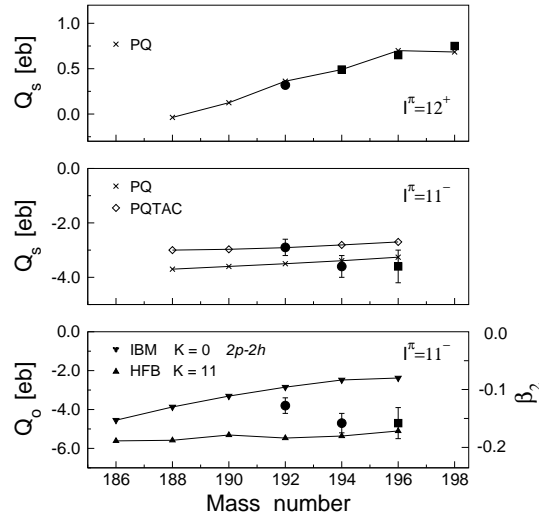


Fig. 4. Experimental spectroscopic quadrupole moments in light lead nuclei for the 12^+ and 11^- states, from present work (full circles) and from [17,21] (full squares) are compared in the two upper panels to the pairing plus quadrupole (PQ) and pairing plus quadrupole tilted axis cranking (PQTAC) calculations. In the lower panel, experimental intrinsic quadrupole moments for the 11^- states are compared to Hartree Fock Bogoliubov mean-field [31] and interacting boson model [11, 32] calculations (see text). The β_2 deformation parameters (vertical scale on the right side of this panel) were calculated for $A=192$. The theoretical values are connected by lines in order to guide the eye.

The spectroscopic quadrupole moments of the 11^- and 12^+ states in Pb nuclei, including the values determined in the present study, are shown in Fig. 4. The 12^+ states with the $1i_{13/2}^2$ two-quasineutron configuration have rather small quadrupole moments, which are decreasing with the decrease of the neutron number. The $|Q_s|$ values of the 11^- states are about an order of magnitude higher, indicating deformed shapes associated with the $\pi 3s_{1/2}^{-2}1h_{9/2}1i_{13/2}$ intruder configuration. We

note that they are identical in $^{194,196}\text{Pb}$, while the $|Q_s|$ value in ^{192}Pb is slightly lower, what could indicate a smaller deformation. It is worthwhile to note that this is also supported by the recently reported $B(E3)$ strengths for the $11^- \rightarrow 8^-$ transition, which decrease from 26(2) W.u. in ^{194}Pb and 29(4) W.u. in ^{194}Pb [16] to a value of 22(2) W.u. in $^{190,192}\text{Pb}$ [15].

The experimental spectroscopic quadrupole moments are compared in Fig. 4 with the calculations performed with the pairing plus quadrupole tilted axis cranking (PQTAC) model which was used to describe the observed magnetic rotational bands in light lead nuclei [28]. In the calculations, the neutron pairing was taken as $0.75\Delta_{oe}$, with Δ_{oe} the experimental odd-even mass difference. The quadrupole-quadrupole coupling constant, which controls the size of the deformation, has been adjusted in order to reproduce the experimental quadrupole moment of the $\nu(1i_{13/2})^2 12^+$ isomer in ^{194}Pb . For the other isotopes this value was scaled with $A^{-5/3}r_{osc}^{-4}$, where r_{osc} is the oscillator length [28]. The calculations for the 12^+ states were performed essentially within the pairing plus quadrupole (PQ) model, as in these cases there is no tilted angle and rotation. As seen in the Fig. 4, the experimental data are nicely reproduced by these calculations which predict a decrease of the Q_s with the decrease of the neutron number due to the change in the occupation number of the neutron $1i_{13/2}$ orbital. A sign changing is predicted at the ^{188}Pb nucleus where the $i_{13/2}$ neutron excitation changes from a hole-type to a particle-type character. The 11^- states were calculated to be oblate deformed, with a moderate quadrupole deformation parameter varying from $\beta_2 = -0.13$ for ^{188}Pb to $\beta_2 = -0.10$ for ^{196}Pb . Calculations were performed with both the PQ and PQTAC approximations. The PQTAC values, which were obtained by treating the 11^- state as a rotational band-head, are slightly smaller than the PQ values. As seen in Fig. 4, a good description of the experimental quadrupole moments was obtained. The Q_s values in $^{194,196}\text{Pb}$ are in better agreement with PQ calculations, while the measured Q_s in ^{192}Pb is closer to the PQTAC calculation. In the lower panel of Fig. 4 are shown the experimental intrinsic quadrupole moments Q_0 of the 11^- states, obtained by assuming $K=I$ and using the relation

$$Q_s = Q_0 \frac{3K^2 - I(I+1)}{(2I+3)(I+1)} \quad (2)$$

The corresponding quadrupole deformation parameter β_2 was derived with the formula $Q_0 = \frac{3}{\sqrt{5}\pi}ZR^2\beta_2$, where $R = r_0A^{1/3}$ and $r_0 = 1.2$ fm. Quadrupole deformation values of $-0.127(13)$, $-0.156(17)$ and $-0.156(26)$ were calculated for ^{192}Pb , ^{194}Pb and ^{196}Pb , respectively. They are consistent within error bars with an average deformation of $\beta_2(11^-) = 0.146(14)$. The experimental Q_0 are compared with theoretical values derived for the 11^- state in $^{186-196}\text{Pb}$ in the framework of the Hartree-Fock-Bogoliubov (HFB) method with a Skyrme interaction and density-dependent pairing force [31]. The 11^- states were constructed fully self-consistently as two-quasiparticle excitations built on top of the excited 0^+ oblate states. As seen in

Fig. 4, the HFB calculations predict Q_0 values that are very slightly increasing with decreasing N , and deformation parameters varying from -0.17 to -0.19 . Similar deformations were calculated for the 11^- isomers by the method of K -constrained diabatic potential-energy surfaces, using a deformed Woods-Saxon potential [16]. In Fig. 4 are also given for comparison the intrinsic quadrupole moments derived in the framework of the interacting boson model for the unperturbed $2p - 2h$ oblate band in $^{186-196}\text{Pb}$ [11, 32]. They were obtained with the same set of parameters in the IBM Hamiltonian [10], except for the initial energy of the intruder excitations [11]. The IBM values show a more pronounced dependence on the neutron number, and are somewhat smaller than the mean-field calculations. Note however that they are the lower limits for the $|Q_0|$ values, obtained in the assumption that the oblate band is a pure $K=0$ band.

The slightly smaller static quadrupole moment measured for the 11^- state in ^{192}Pb compared to the heavier nuclei $^{194,196}\text{Pb}$, in disagreement with the theoretical predictions for a pure oblate state, can possibly be viewed as an evidence for shape mixing. An increased mixing of spherical and/or prolate configurations might be present in ^{192}Pb either in the structure of the 0_2^+ oblate state on top of which is constructed the broken pair proton excitation, or in the structure of the high K state itself. Note that a complex structure of the 11^- state, involving possible K mixing, was suggested also by the properties of the irregular band structure built above it, as discussed recently by Dracoulis et al. [6].

In summary, the pulsed beam TDPAD method has been applied for precise spectroscopic quadrupole moment determinations in $^{192,194}\text{Pb}$ nuclei. The quadrupole moments for the 11^- and 12^+ isomers in the ^{192}Pb nucleus were measured for the first time, and the quadrupole moment of the 11^- state in ^{194}Pb was remeasured with an increased precision. The systematics of known spectroscopic quadrupole moments in light Pb nuclei illustrates their sensitivity to the complex structure of coexisting states. More experimental data on quadrupole moments is necessary to have more insight into the detailed structure of the quasiparticle excitations built on coexisting minima in neutron-deficient Pb nuclei.

Acknowledgements

The work was supported in part by the Romanian National Authority for Scientific Research, Program of Excellence, Contract No. 05-D11-30. D.L.B. acknowledges Bulgarian Science Fund, grant VUF06/05. Support through the European Community FP6 - Integrated Infrastructure Initiative EURONS contract nr. RII3-CT-2004-506065 is acknowledged.

References

- [1] J.L. Wood, et al., Phys. Rep. 215 (1992) 101.
- [2] R. Julin, K. Helariutta, M. Muikku, J. Phys. G 27 (2001) R109.
- [3] P. Dendooven, et al., Phys. Lett. B 226 (1989) 27.
- [4] A.N. Andreyev, et al., Nature (London) 405 (2000) 430.
- [5] G.D. Dracoulis, A.P. Byrne, A.M. Baxter, Phys. Lett. B 432 (1998) 37.
- [6] G.D. Dracoulis, et al., Phys. Rev. C 69 (2004) 054318.
- [7] T. Grahn, et al., Phys. Rev. Lett. 97 (2006) 062501.
- [8] J. Pakarinen, et al., Phys. Rev. C 75 (2007) 014302.
- [9] C. De Coster, B. Decroix, K. Heyde, Phys. Rev. C 61 (2000) 067306.
- [10] R. Fossion, K. Heyde, G. Thiamova, P. Van Isacker, Phys. Rev. C 67 (2003) 024306.
- [11] V. Hellemans, R. Fossion, S. De Baerdemacker, K. Heyde, Phys. Rev. C 71 (2005) 034308.
- [12] W. Nazarewicz, Phys. Lett. B 305 (1993) 195.
- [13] M. Bender, P. Bonche, T. Duguet, P.-H. Heenen, Phys. Rev. C 69 (2004) 064303.
- [14] J.L. Egido, L.M. Robledo, R. Rodriguez-Guzman, Phys. Rev. Lett. 93 (2004) 082502.
- [15] G.D. Dracoulis, et al., Phys. Rev. C 63 (2001) 061302(R).
- [16] G.D. Dracoulis, et al., Phys. Rev. C 72 (2005) 064319.
- [17] N.J. Stone, Atomic Data and Nuclear Data Tables 90 (2005) 75.
- [18] M. Ionescu-Bujor, et al. Phys. Rev. C 70 (2004) 034305.
- [19] K. Vyvey, et al., Phys. Rev. C 65 (2002) 024320.
- [20] K. Vyvey, et al., Phys. Rev. Lett. 88 (2002) 102502.
- [21] K. Vyvey, et al., Eur. Phys. J. A 22 s01 (2004) 1.
- [22] C.M. Baglin, Nuclear Data Sheets 84 (1998) 717.
- [23] B. Singh, Nuclear Data Sheets 107 (2006) 1531.
- [24] Z. Chunmei, W. Gongqing, T. Zhenlan, Nuclear Data Sheets 83 (1998) 145.
- [25] Z. Chunmei, Nuclear Data Sheets 95 (2002) 59.
- [26] M.R. Schmorak, Nuclear Data Sheets 75 (1995) 667.
- [27] A.J.M. Plompen, et al., Nucl. Phys. A 562 (1993) 61.

- [28] S. Frauendorf, Nucl. Phys. A 677 (2000) 115.
- [29] E. Dafni, R. Bienstock, M.H. Rafailovich and G.D. Sprouse, At. Data Nucl. Data Tables 23 (1979) 315.
- [30] E. Dafni et al., Nucl. Phys. A 394 (1983) 245.
- [31] N.A. Smirnova, P.-H. Heenen, G. Neyens, Phys. Lett. B 569 (2003) 151.
- [32] V. Hellemans, private communication.